Flow and Diffusion of Gases Through Porous Substrates

An experimental study of simultaneous flow and binary diffusion through four porous catalyst substrates was conducted in the range of pressure from 1 to 3 bar absolute. Experiments on the flow of pure gases and isobaric binary diffusion were carried out on the same catalyst substrates. The differential equations describing simultaneous flow and diffusion in the form of the Chapman-Enskog first-order approximations were solved analytically, taking into account the variation of viscosity with composition. The parameters for the diffusion and flow processes were found from separate experiments on flow and diffusion, from experiments on nonisobaric flow and diffusion, and from composition transients in fixed beds. There was good agreement between theory and experiment except for permeability experiments at low pressures, where significant differences were found.

Z. M. Allawi and D. J. Gunn
Department of Chemical Engineering
University College of Swansea
Singleton Park, Swansea
SA2 8PP United Kingdom

Introduction

The rate of transport of gases in catalysts and other porous solids depends upon: the nature of the diffusing gases; the conditions causing the transport, whether due to reaction or pressure differences; and the size and distribution of pores within the catalyst, as well as the temperature and pressure of operation. If the pore size is sufficiently small, Knudsen diffusion will be dominant; at higher pressures in larger pores, bulk diffusion will be the dominant mode.

There have been a number of analyses of the phenomena of bulk diffusion and Knudsen flow in porous solids that are related, in some cases, to studies of flow and diffusion in capillary tubes. For example Scott and Dullien (1962) studied gas flow through a straight capillary, and transition flow and diffusion in porous media under isothermal and isobaric conditions. Evans et al. (1961) treated the porous medium as an assembly of large particles to give equations for the dusty gas model. The theoretical equations established from considerations of this model were similar to those of Scott and Dullien. Several of the comparisons between these models and experimental measurements have been complicated by the influence of surface diffusion (Satterfield and Cadle, 1968; Asaeda et al., 1981).

Mason et al. (1967) have suggested that in the case of nonisobaric diffusion the total flux of a component is the sum of the diffusive flux and an additional independent viscous contribution. A particular form for this equation was suggested by Gunn and King (1969).

Abed and Rinker (1974) and later Chen and Rinker (1979) presented a similar set of differential equations for diffusion and flow based upon the dusty gas model, but with some modifications. The equations were integrated numerically and compared with experimental measurements for the flow and diffusion of helium and nitrogen through porous solids. Otani et al. (1965) measured diffusion and flow through Vycor glasses of different pore sizes.

It apparently has not proved possible to use parameters characterizing flow and diffusion in equations describing the combined phenomena without introducing additional correction factors (Abed and Rinker, 1974; Chen and Rinker, 1979), and it is not known whether this requirement is a defect of the theory or is caused by the intrusion of experimental error and errors due to numerical integration of the equation.

The object of this investigation was to examine the dependence of flow and diffusion through a number of porous substrates upon pressure and gas concentration for a number of gases using a diffusion cell of the Wicke-Kallenbach type; diffusion through the substrates had been previously examined by other techniques. The experiments were carried out for flow and diffusion separately as well as together under conditions such that Knudsen effects were either significant or dominant, at least for some experiments. The analysis of the experimental results was aided by expressing the theoretical dependence of the fluxes upon pressure and composition in the form of a small

*Correspondence concerning this paper should be addressed to D. J. Gunn.

number of equations that were established by analytical integration of the basic ordinary differential equations. The experiments were carried out for six gases of relative molecular masses from 2 to 44 so that the effect of the molecular nature of the diffusing and permeating gases upon the transport parameters could be examined.

Theory

The basic differential equation that describes binary diffusion in porous solids is

$$J_1 = \frac{-D_{12}}{RT}\frac{dP_1}{dx} + y_1(J_1 + J_2) \tag{1}$$

where the first term on the righthand side is the flux due to molecular diffusion while the second term is the transport due to bulk flow. The differential equation describing Knudsen diffusion is,

$$J_1 = \frac{-K_1}{RT}\frac{dP_1}{dx} \tag{2}$$

The effective Knudsen diffusion coefficient K_1 is related to the absolute temperature T, the effective radius of pores in the solid r_e, and the relative molecular mass of the diffusing gas by,

$$K_1 = A\, r_e \sqrt{\frac{T}{M_1}} \tag{3}$$

where A is a constant for the medium that does not depend upon the gas.

In given ranges of pore size and gas pressure, either Knudsen flow or bulk diffusion may dominate. As gas pressure is reduced, the relative importance of Knudsen flow increases and the numerical value of the coefficient for bulk diffusion that changes as $1/p$, increases relative to the Knudsen coefficient. On the other hand, if pore size is increased bulk diffusion becomes more important, and the Knudsen coefficient increases relative to the bulk diffusion coefficient.

A form for the diffusion coefficient in the transition region with the correct asymptotes characterizing bulk diffusion and Knudsen diffusion has been derived by a variety of arguments. Thus Pollard and Present (1948) used momentum transfer arguments, while Scott and Dullien (1962) applied elementary momentum transport theory in gases to diffusion in the transition region. Evans et al. (1961) formally treated the solid matrix as particles in a "dusty gas" in which the dust particles are held stationary. In extending this concept to transition region diffusion, they together with Scott and Dullien and Pollard and Present, confirmed the applicability of the Bosanquet interpolation formula, Eq. 4. Evidently this formula may be derived on the basis of several different arguments. The formula is

$$\frac{1}{D_1} = \frac{1}{D_{12}} + \frac{1}{K_1} \tag{4}$$

The correct asymptotic form of the transport equation may be obtained by an even simpler argument. The driving force for diffusion, the partial pressure gradient dP_1/dx, is the macroscopic manifestation of molecular momentum changes in the gas. Of this quantity a proportion dP_{12}/dx is a measure of the probability of molecular momentum changes under conditions of bulk diffusion, and a proportion dP_{1K}/dx is a measure of the probability of molecular momentum changes due to molecular impacts with the substrate under conditions of free molecular flow. An individual molecule will undergo a sequence of impacts, some intermolecular and others of a free molecular nature, and the molar fluxes are then given as the sums of the molecular sequences for all molecules. At the steady state the rate of diffusion may be expressed.

$$J_1 = \frac{-D_{12}}{RT}\frac{dP_{12}}{dx} + y_1(J_1 + J_2) = \frac{-K_1}{RT}\frac{dP_{1K}}{dx} \tag{5}$$

and since

$$\frac{dP_1}{dx} = \frac{dP_{12}}{dx} + \frac{dP_{1K}}{dx} \tag{6}$$

on expressing Eq. 5 in terms of the partial pressure gradient dP_1/dx, the following equation is obtained.

$$J_1 = \frac{-D_{12}K_1}{RT(D_{12} + K_1)}\frac{dP_1}{dx} + \frac{y_1K_1}{(D_{12} + K_1)}(J_1 + J_2) \tag{7}$$

This is the equation derived from considerations of molecular diffusion in the dusty gas by Evans et al. and by Scott and Dullien from molecular momentum balances. The equation gives the correct limiting behavior in that when D_{12} becomes large relative to K_1, as at low pressures because of the dependence upon $1/p$, the equation for Knudsen flow is generated; while when K_1 becomes large relative to D_{12}, as in large pores, the equation for bulk diffusion is found. The form of Eq. 7 is apparently insensitive to the detailed nature of the molecular mechanisms that have been considered in deriving it, and its utility may be due to its satisfactory asymptotic form.

Nonisobaric Flow and Diffusion

According to Mason et al. (1967), the several different approaches to the problem of gas transport in porous media may be unified on the basis of the kinetic theory of gases. The dusty gas model provides a means of adapting the Chapman-Enskog solution to porous media. Mean free path procedures, when carried to high orders of approximation yield results in agreement with the Chapman-Enskog treatment, and momentum-transfer descriptions of diffusion give the same formula for the diffusion coefficient as that given by the Chapman-Enskog first approximation. For isobaric diffusion in porous media the common formula is the asymptotic form, Eq. 4.

For nonisobaric flow and diffusion, the first-order Chapman-Enskog approximation for diffusive transport is given by one equation and viscous flow by another, and the two are entirely independent, without cross terms. When deviations from the Maxwellian distribution of velocities are followed to the second order of small quantities, the equations become much more complex and are no longer independent. Almost all of the additional terms may be shown to be unnecessary, either because they are small compared to first-order terms in cases of fundamental interest, or because they are inherent in the use of asymptotic procedures. To include viscous flow and diffusion with depen-

dent terms apparently gives an unneeded, ultrarefined description (Mason et al., 1967).

Viscous flow through porous media may be characterized by the Darcy equation and the Darcy coefficient of permeability C. Thus for component 1:

$$J_{1(V)} = \frac{-CP}{\mu RT} y_1 \frac{dP}{dx} \tag{8}$$

If the viscous flow is independent of the diffusive, then the total flux $J_{1(T)}$ is the sum of the diffusive given by Eq. 7 and the viscous contribution of Eq. 8

$$J_{1(T)} = \frac{-D_{12}K_1}{RT(D_{12} + K_1)} \frac{dP_1}{dx} + \frac{y_1 K_1}{(D_{12} + K_1)} (J_1 + J_2) - \frac{CP}{\mu RT} y_1 \frac{dp}{dx} \tag{9}$$

By writing Eq. 9 for the second component of the binary system and rearranging, the total transport rates for each component are found. For component 1

$$J_{1(T)} = \frac{-K_1 D_{12} P}{RT(y_2 K_1 + y_1 K_2 + D_{12})} \frac{dy_1}{dx} - \left[\frac{y_1 K_1 (D_{12} + K_2)}{RT(y_2 K_1 + y_1 K_2 + D_{12})} + \frac{CPy_1}{\mu RT} \right] \frac{dp}{dx} \tag{10}$$

an equation that has been given by Gunn and King (1969).

In considering the integration of Eq. 10, it may be remarked that the binary diffusion coefficient in the porous medium D_{12} appears in both the numerator and denominator of the first two terms on the righthand side, and in the first term in particular, the product $D_{12}P$ is substantially independent of pressure. The effect of the small concentration dependence of D_{12}, and the larger pressure dependence of the same coefficient will partially cancel out. However, as the concentration dependence is weak, the ratio in the first two terms on the righthand side will be sensibly independent of concentration, but will be sensibly independent of pressure only if pressure variation within the pellet is small compared to the mean pressure. This condition is implicit in the succeeding development.

Given these conditions, the remaining difficulty is the concentration dependence of the gas viscosity μ. To maintain the correct asymptotic conditions, Eq. 10 may be expressed for components 1 and 2 by the following equations:

$$J_{1(T)} = \frac{-K_1 D_{12} P}{RT(y_2 K_1 + y_1 K_2 + D_{12})} \frac{dy_1}{dx} - \left[\frac{y_1 K_1 (D_{12} + K_2)}{RT(y_2 K_1 + y_1 K_2 + D_{12})} + \frac{CP(D_{12} + K_2) y_1}{\mu_1 RT(y_2 K_1 + y_1 K_2 + D_{12})} \right] \frac{dp}{dx} \tag{11}$$

$$J_{2(T)} = \frac{-K_2 D_{12} P}{RT(y_2 K_1 + y_1 K_2 + D_{12})} \frac{dy_2}{dx} - \left[\frac{y_2 K_2 (D_{12} + K_1)}{RT(y_2 K_1 + y_1 K_2 + D_{12})} + \frac{CP(D_{12} + K_1) y_2}{\mu_2 RT(y_2 K_1 + y_1 K_2 + D_{12})} \right] \frac{dp}{dx} \tag{12}$$

In these equations $\mu_1(y_2K_1 + y_1K_2 + D_{12})/(D_{12} + K_2)$ has been written for μ in the equation for component 1, and $\mu_2(y_2K_1 + y_1K_2 + D_{12})/(D_{12} + K_1)$ has been written for μ in the equation for component 2 so that the asymptotic conditions are fulfilled. Since both expressions for the viscosity should be the same, on equating one to the other we obtain,

$$\frac{\mu_1}{\mu_2} = \frac{D_{12} + K_2}{D_{12} + K_1} \tag{13}$$

For conditions under which viscous flow rather than Knudsen flow is important, D_{12} is small compared to K_2 or K_1, so that the ratio of viscosities

$$\frac{\mu_1}{\mu_2} \approx \frac{K_2}{K_1} = \sqrt{\frac{M_1}{M_2}} \tag{14}$$

where the final equality follows from Eq. 3. The proportionality between the ratio of viscosities and the square root of the ratio of molecular masses is in agreement with predictions of the kinetic theory of gases, and therefore Eqs. 11 and 12 are satisfactory to this extent.

The two expressions for the viscosity are also equivalent to Eq. 15, which may be derived from either by use of Eq. 13.

$$\mu = \frac{\mu_1 \mu_2 (y_2 K_1 + y_1 K_2 + D_{12})}{(D_{12} + K_1)\mu_1 y_2 + (D_{12} + K_2)\mu_2 y_1} \tag{15}$$

We will compare the predictions of this equation with the comparative dependences suggested by Herning later in the paper.

$$\mu = \frac{\mu_1 y_1 M_1^{1/2} + \mu_2 y_2 M_2^{1/2}}{y_1 M_1^{1/2} + y_2 M_2^{1/2}} \tag{16}$$

Both Eqs. 15 and 16 approach the limits of μ_1 as $y_1 \rightarrow 1$ and of μ_2 as $y_2 \rightarrow 1$, with a similar monotonic functional dependence of viscosity upon composition and molecular mass introduced into Eq. 15 by Eq. 14.

Equations 11 and 12 take the form, respectively:

$$J_{1(T)} = \frac{A_1}{ay_1 + b} \frac{dy_1}{dx} + \frac{A_2 y_1}{ay_1 + b} \frac{dp}{dx} \tag{17}$$

$$J_{2(T)} = \frac{B_1}{ay_1 + b} \frac{dy_1}{dx} + \frac{B_2 y_2}{ay_1 + b} \frac{dp}{dx} \tag{18}$$

where A_1, A_2, B_1, B_2, a, and b are substantially constant over the pellet, bearing in mind the condition that departures of pressure from the mean pressure in the pellet are small.

An expression for the dependence of pressure upon composition in the pellet may be arranged by use of the ratio $\alpha = -J_{1(T)}/J_{2(T)}$ to eliminate $J_{1(T)}$ and $J_{2(T)}$. On setting up the differential

equation and integrating,

$$P_2 - P_1 = \frac{D_{12}(K_1 - \alpha K_{12})\bar{P}}{(D_{12} + K_{12})\left(K_1 + \frac{CP}{\mu_1}\right) - \alpha(D_{12} + K_1)\left(K_{12} + \frac{CP}{\mu_2}\right)} \cdot \ln\left[\frac{1 + \beta y_{1(1)}}{1 + \beta y_{1(2)}}\right] \quad (19)$$

where

$$\beta = [(D_{12} + K_2)(K_1 + C\bar{p}/\mu_1) - \alpha(D_{12} + K_1)(K_2 + C\bar{p}/\mu_2)]/\alpha(D_{12} + K_1)(K_2 + C\bar{p}/\mu_2) \quad (20)$$

$\bar{p}$ is the mean pressure, and $y_{1(1)}$ and $Y_{1(2)}$ are the concentrations of component 1 at each face of the pellet. Equation 19 allows the pressure difference to be calculated for set values of α, $\bar{p}$, $y_{1(1)}$, and $y_{1(2)}$, or a value of concentration may be calculated from other fixed variables, or the equation may be solved as a transcendental equation for α.

If the gradient dp/dx is eliminated from Eqs. 17 and 18, the total flux of each component may be found. For component 1

$$J_{1(T)} = \frac{\alpha D_{12} C\bar{p}^2}{RTL(K_2 - K_1)} \cdot \left[\frac{K_2/\mu_1 - K_1/\mu_2}{K_1 + C\bar{p}/\mu_1 - \alpha(K_1 + C_p/\mu_2)}\right] \cdot \ln\left[\frac{(K_2 - K_1)y_{1(1)} + K_1 + D_{12}}{(K_2 - K_1)y_{1(2)} + K_1 + D_{12}}\right] + \frac{\alpha(K_1 + C\bar{p}/\mu_1)(K_2 + C\bar{p}/\mu_2)(P_1 - P_2)}{RTL(\alpha(K_2 + C\bar{p}/\mu_2) - (K_1 + C\bar{p}/\mu_1)} \quad (21)$$

with either α or $(P_1 - P_2)$ established from Eq. 19, the flux $J_{1(T)}$ is given as a function of end compositions, and either $(P_1 - P_2)$ or α by Eq. 21.

Equations 19 and 21 were used in the experimental program to examine experiments on simultaneous diffusion and flow, but two more limited applications of these equations were also examined in experiment. In the first additional type, that of isobaric diffusion, a zero pressure difference in Eq. 19 gives

$$\alpha = \frac{K_1}{K_2} = \sqrt{\frac{M_2}{M_1}} \quad (22)$$

while this condition when set in Eq. 21 gives

$$J_1 = \frac{D_{12}K_1 p}{RTL(K_2 - K_1)} \ln\frac{(K_2 - K_1)y_{1(1)} + K_1 + D_{12}}{(K_2 - K_1)y_{1(2)} + K_1 + D_{12}} \quad (23)$$

an expression that agrees with those of Scott and Dullien (1962) and Evans et al. (1961).

In the second additional type of experiment, that of flow of a single gas under a pressure difference, the molar flow is given by

$$J_{1(T)} = \frac{P_1 - P_2}{RTL}(K_1 + C\bar{p}/\mu_1) \quad (24)$$

A graph of $J_{1(T)}RTL/(P_1 - P_2)$ against the mean pressure $(\frac{1}{2})(P_2 + P_1)$ should give a linear plot of intercept K_1 and gradient C/μ. Equation 24 is not limited by the requirement that ΔP should not be large compared to $\bar{p}$, since this limitation applies to Eqs. 19 and 21 because of the pressure dependence of the binary diffusivity.

Experimental Method

The diffusion and flow experiments were carried out in a cell similar to that employed by Wicke and Kallenbach. Figure 1 is a diagram of the arrangement for gas permeabilities. High-purity gas from the cylinder passed through the porous substrate into the vacuum pump and the pressure difference was measured by manometers controlled by the valves VM1–VM3. The pressure in the lower compartment was measured either by a Vacuostat MG (a small McLeod gauge) or by a mercury manometer of which one leg was evacuated and sealed. The experiments were

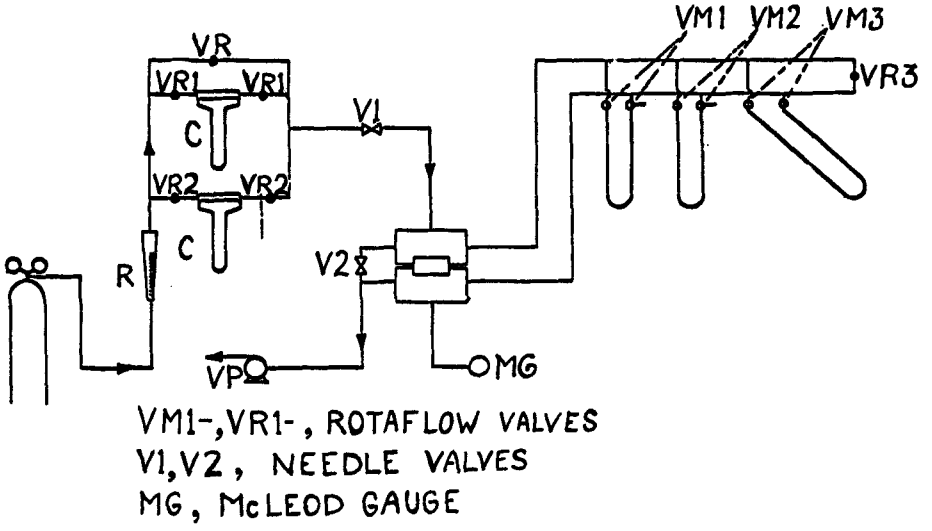

Figure 1. Experimental arrangement for permeability measurements.

carried out at mean pressures up to 1,200 mm Hg (159.6 kPa) with argon, helium, hydrogen, nitrogen, and carbon dioxide.

The experimental arrangement for diffusion experiments is shown in Figure 2. The flow rates of two high-purity gases were measured by rotameters in each side of the diffusion cell. Samples of the outlet of each stream were collected in a sample loop and injected into the chromatographic column once steady state had been reached.

The properties shown in Table 1 were obtained by England (1971), who measured pore radii distributions by mercury porosimetry. The pore size distribution for SA203 appeared predominantly unimodal, while all three LA grades showed a significant bimodality in the pore size distributions.

Results and Discussion

Each set of permeability experiments was carried out for absolute pressures between 1 and 1,300 mm Hg (0.133 ms 173 kPa). When examined according to Eq. 24, the dependence of permeability upon mean pressure was predominantly linear, but in some cases with a pronounced departure from linearity in the range from 1 to 80 mm Hg (0.133 to 10.6 kPa). The deviation from linearity was most pronounced in fine-pore material and for gases of low molecular mass. Figure 3 shows the permeability of the substrate with the finest pores, LA617, as a function of mean pressure for the flow of hydrogen where the departure from linearity was most pronounced. Barrer (1963) has reported some experiments carried out by Hirsch on sintered glass membranes that show a similar fall in permeability at low pressures. The dependence of permeability upon mean pressure in capillary tubes shows a minimum at low pressures, and this effect is not predicted by the first-order Chapman-Enskog treatment; Mason et al. (1967) consider that the minimum may be taken into account by higher order approximations. Higher order approximations may be necessary to describe the effect in terms of kinetic theory for porous media also. However in this set of experiments the dependence of permeability upon mean pressure was predominantly linear, and the Knudsen diffusivity and the Darcy permeability may be found graphically.

An estimate of the Knudsen diffusivity may be found from pore size distributions of the substrates

$$\bar{r} = \frac{\int_0^\infty r dV}{\int_0^\infty dV} \tag{25}$$

where the variable V represents the volume of mercury penetration. The values of $\bar{r}$ calculated from this equation are shown in Table 1. The Knudsen diffusivity K_1 may be calculated from $\bar{r}$ by means of the equation

$$K_1 = \frac{2\epsilon}{3\tau}\sqrt{\frac{8RT}{\pi M_1}} \tag{26}$$

where ϵ is the particle porosity, also obtained by mercury porosimetry, and τ is the tortuosity factor. In this application the value of τ was found from experimental measurements of isobaric diffusion to be described. The values of K_1 found from intercepts of the graphs, from Eq. 26, and the values of the Darcy permeability C found from gradients of the graphs are shown in Table 2.

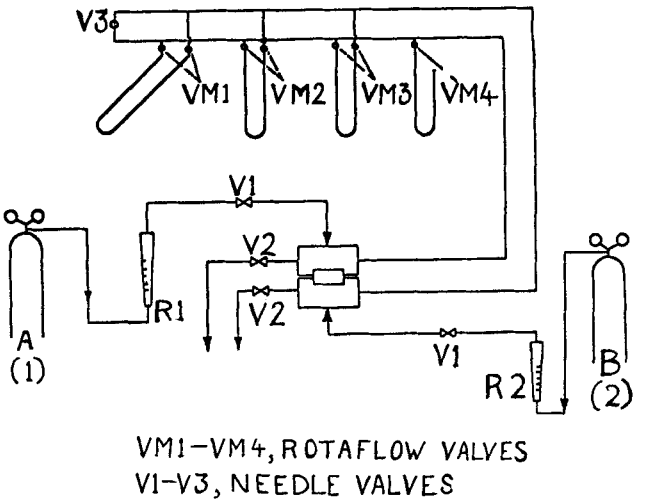

Figure 2. Experimental arrangement for isobaric and nonisobaric diffusion.

This table illustrates several points of importance. It may be seen that the Darcy permeabilities C are independent of the nature of the permeating gas—a condition that must be fulfilled if the analysis is to have physical significance—but differ for the particular substrates. Permeabilities vary by a factor of 50 from the fine-pore, high surface area LA617 to the wide-pore, low surface area SA203. It is also evident that values of the Knudsen coefficient found from the graphs agree closely with values of the Knudsen coefficient K_1 that have been calculated from Eq. 26. This agreement between the two sets of Knudsen coefficients establishes that Knudsen coefficients found by the graphical procedure are proportional to the inverse of the square root of the relative molecular mass, as required by Eq. 26, and show that tortuosity factors for Knudsen flow are similar to those found for isobaric diffusion.

Isobaric and nonisobaric diffusion

The experimental fluxes for each experiment were calculated from material balances using the measured flow rates and the composition of the gas streams found by chromatographic analysis. If y_1 is the volume (mole) fraction of component 1 in the stream of gas leaving the pellet from cylinder A, and y_2 is the volume (mole) fraction of component 2 in the stream leaving the pellet from cylinder B, the flux ratio is given by,

$$\frac{J_1}{J_2} = \frac{y_1[V_B(1-y_2) - y_2V_A]}{y_2[V_A(1-y_1) - y_1V_B]} \tag{27}$$

Table 1. Physical Properties of Catalyst Substrates

Property	Particle Grade			
	SA203	LA617	LA622	LA623
Particle porosity, %	35.5	59.0	58.0	58.0
Surface area, m^2/g	0.075	37.7	18.4	8.12
Material density, g/mL	3.55	3.10	3.01	3.04
Particle bulk density, g/mL	2.54	1.28	1.26	1.24
Mean pore volume, mL/g	0.114	0.447	0.443	0.478
Avg. pore radius, μm	6.50	0.900	1.46	2.19

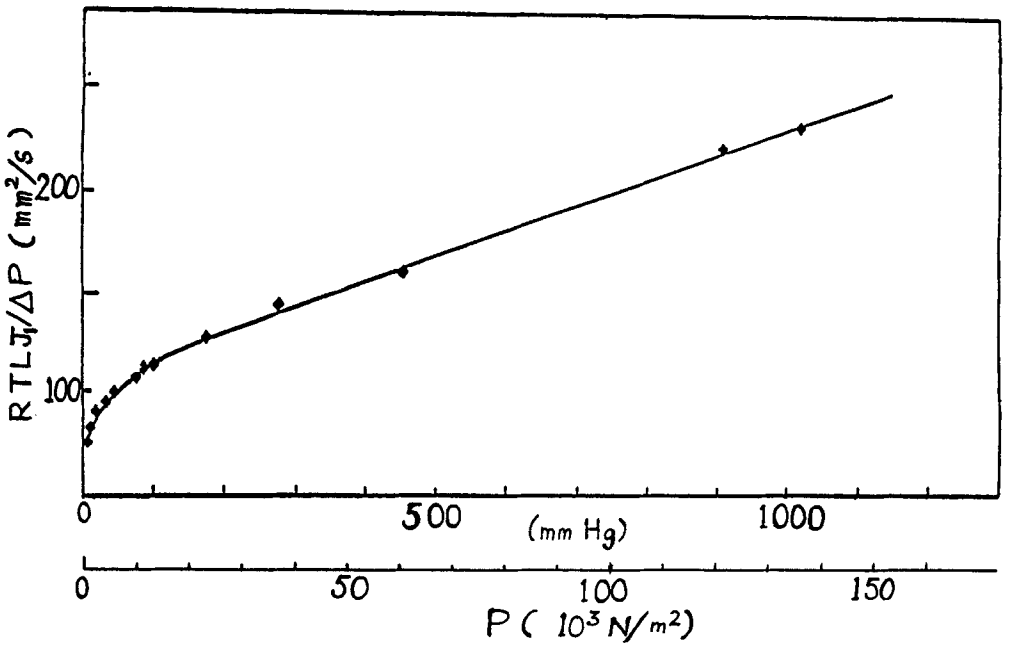

Figure 3. Experimental dependence of permeability upon mean pressure for hydrogen through LA617.

where V_A is the volume (molar) flow rate from cylinder A, and V_B is the volume (molar) flow rate from cylinder B, Figure 2.

The values of D_{12}, K_1, and K_2 were found from the dependence of the fluxes J_1 and J_2. For each pellet type and pairs of counterdiffusing gases, three or four separate experiments were carried out on different samples of pellets. A single set of parameters was found from the experiments on one pellet type by finding the least sum of squares according to the formula

$$F = \sum_{i=1}^{n} \left(\frac{J_{1\text{theory}} - J_{1\text{exp}}}{J_1 \text{ exp}} \right)^2 + \sum_{i=1}^{n} \left(\frac{J_{2\text{theory}} - J_{2\text{exp}}}{J_2 \text{ exp}} \right)^2 \qquad (28)$$

The parameters in Eq. 23 were adjusted in an automatic computer routine until the sum of squares, Eq. 28, was a minimum. The parameters corresponding to this minimum were the best values given by that experiment. The three parameters D_{12}, K_1, and K_2 as well as the flux ratios for the experiments on isobaric diffusion are shown in Table 3.

The ratio of counterdiffusing fluxes was compared to the inverse ratio of the square root of the molecular masses predicted from kinetic theory. The agreement was close, with a mean deviation of 0.65%.

Experiments on non-isobaric diffusion and flow were analyzed by Eqs. 19 and 21. The value of the flux ratios was found from Eq. 19 by means of a mixed Secant-Newton-Raphson routine for finding the roots of transcendental equations. The theoretical value of $J_{1(T)}$ was found from Eq. 21, and therefore the theoretical value of $J_{2(T)}$ could be calculated from α and $J_{1(T)}$. The sum of the squares of the experimental estimates about the theoretical predictions was found by means of Eq. 28 and the same automatic routine for parameter estimation was employed to find the parameters D_{12}, K_1, K_2, and C associated with each experiment on nonisobaric diffusion. Each set of parameters corresponded to some four to nine experiments in which the fluxes of flowing and counterdiffusing gases were measured at a number of different pressure conditions.

The parameters are shown in Table 3.

Figure 4 shows the experimental dependence upon pressure difference of the flux of argon diffusing against the pressure gradient and a counterflux of carbon dioxide for pellet grades

Table 2. Knudsen Diffusivities and Darcy Permeabilities for Porous Substrates

	Pellet Grade											
	SA203			LA617			LA622			LA623		
Gas	K_1 graph	K_1 Eq. 26	C	K_1 graph	K_1 Eq. 26	C	K_1 graph	K_1 Eq. 26	C	K_1 graph	K_1 Eq. 26	C
H_2	496.7	484.3	3.40	57.7	79.1	0.0808	161.6	138.8	0.521	267.0	243.0	0.959
He	—	—	—	—	—	—	101.8	98.1	0.541	178.0	207.1	0.933
N_2	—	—	—	15.4	21.1	0.0799	46.2	37.1	0.515	80.6	78.3	0.894
CH_4	184.7	171.2	3.28	—	—	—	50.9	49.1	0.518	101.20	103.6	0.875
Ar	104.6	108.3	3.00	12.7	17.7	0.0737	35.3	31.0	0.523	62.3	65.5	0.962
CO_2	—	—	—	12.2	16.9	0.0702	33.1	29.6	0.520	59.0	62.5	0.943

K_1 mm²/s; $C \times 10^7$ mm²

Table 3. Estimates of Coefficients for Binary and Knudsen Diffusion and Darcy Permeability

Pellet Grade; Gas Pair	Exp.*	Diffusivities, mm^2/s D_{12}	K_1	K_2	Darcy Permeability $C \times 10^7$ mm^2
SA203					
H_2–Ar	NI	5.53	620	250	3.13
H_2–Ar	I	5.17	591.8	131.7	—
H_2–N_2	I	5.03	642.3	177.5	—
He–Ar	I	5.50	464.1	144.6	—
LA617					
He–Ar	NI	4.26	41.0	14.9	0.090
N_2–CO_2	NI	1.12	15.26	10.75	0.083
N_2–CO_2	I	1.30	16.0	10.86	—
Ar–CO_2	NI	0.877	14.53	12.23	0.076
Ar–CO_2	I	1.04	13.36	12.49	—
LA622					
H_2–Ar	NI	5.965	138.6	37.78	0.52
H_2–N_2	I	5.82	162.8	45.9	—
He–Ar	NI	4.580	119.0	40.08	0.404
CH_4–Ar	Ni	1.915	54.13	29.01	0.513
CH_4–Ar	I	1.746	54.4	35.2	—
N_2–CO_2	NI	1.368	31.53	27.95	0.450
Ar–CO_2	NI	1.322	33.35	32.20	0.520
Ar–CO_2	I	1.172	37.9	37.2	—
LA623					
H_2–N_2	NI	8.614	270.7	84.31	0.906
H_2–Ar	I)	7.735	227.6	50.1	—
He–Ar	NI	8.246	154.4	65.78	1.18
He–Ar	I	8.345	193.	62.5	—
CH_4–Ar	NI	2.593	94.01	50.04	0.902
N_2–CO_2	NI	1.514	84.35	64.46	0.883
Ar–CO_2	NI	1.500	61.05	59.65	0.920
Ar–CO_2	I	1.577	65.7	63.6	—

*I, isobaric diffusion experiment
NI, nonisobaric flow and diffusion experiment

LA617, LA622, and LA623. The experimental points are shown, and the full lines illustrate the theoretical solution of Eqs. 19 and 21. Figure 5 shows the experimental dependence of the flux of nitrogen counterdiffusing against carbon dioxide and the pressure gradient for the same grades of pellet.

The agreement between experiment and theory is typical. The variance of the experimental points about the theoretical equations may be considered to have two components, one due to experimental error, and the second due to the accuracy of the model. The component of variance due to experimental error may be assessed by performing replicate experiments. Five replicate experiments were included in the experimental program to give 2.22×10^{-3} as the error variance, compared with the total variance of 3.047×10^{-3}. The variance ratio test (Brownlee, 1953) may be used to assess the probability that the total variance was due to experimental error. The test gave a probability >0.2 that the total variance was due to experimental error, corresponding to the probability that the model gave a good representation of the experimental data.

The coefficients C for the Darcy permeability may be seen to be independent of the gases in the permeability and the nonisobaric diffusion experiments, although clearly different for the four grades of porous substrate. The mean values and standard deviations for each of the four grades are shown in Table 4.

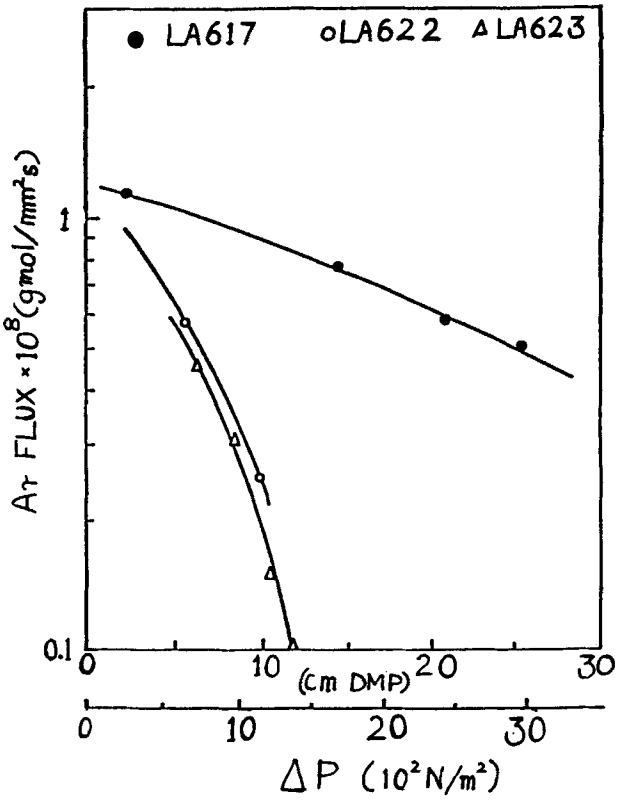

Figure 4. Experimental dependence of argon flux upon opposed pressure differences in nonisobaric diffusion of Ar-CO_2.

It is clear that both sets of mean values shown in Table 4 are consistent with estimates from permeability experiments as shown in Table 3, and with estimates of C found from experiments on flow and nonisobaric diffusion in Table 2. The standard deviations indicate that a better reproducibility of estimates for the Darcy permeability was given by the permeability experiments than by experiments on nonisobaric diffusion. The main reason for the better reproducibility was the wider range of pressures examined in the permeability experiments. The values of C found from permeability experiments lie within mean and one standard deviation of the corresponding experiments on nonisobaric diffusion without bias toward one type of experiment or the other.

The effective binary diffusivity in the porous medium D_{12} may be related to the binary diffusivity in a still fluid $D_{12(m)}$ by

$$D_{12} = \frac{\epsilon}{\tau} D_{12(m)} \tag{29}$$

where ϵ is the particle porosity and τ is the tortuosity factor. As both ϵ and τ are independent of the nature of the diffusing gases, D_{12} should change in the same way as $D_{12(m)}$ when the diffusing gases are changed. The dependence of the binary diffusivity D_{12} upon the molecular characteristics of the diffusing species may be compared with experimental values (Reid and Sherwood, 1958; Reid et al., 1975).

The estimates for the binary diffusivity shown in Tables 2 and 3 have been plotted against the molecular binary diffusivities in Figure 6. The linear dependence of ordinate upon abscissa is

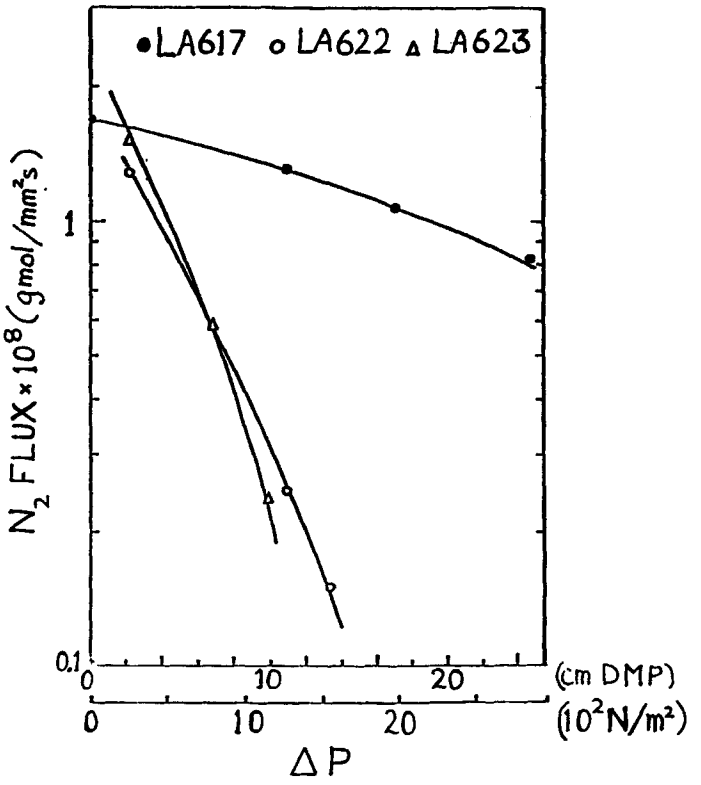

Figure 5. Experimental dependence of nitrogen flux upon opposed pressure differences in nonisobaric diffusion of N_2-CO_2.

faithfully reflected by Figure 6, and therefore the binary diffusivity in the porous medium shows the dependence upon the properties of the diffusing gases that would be expected from the kinetic theory of gases when applied to porous media, at least in the first-order approximation.

Figure 6 also shows estimates of the binary diffusivity obtained by two different transient methods. Gunn and England (1971) estimated the effective diffusivities of catalyst substrates SA203, LA617, LA622, and LA623 from the experimental frequency response of a fixed bed. Bashi and Gunn (1977) estimated the diffusivity of LA622 from the pulse response of a fixed bed. The agreement between estimates from the dynamic methods and the steady state methods described in this paper is excellent.

According to Eq. 3 the influence of the permeating gas upon the Knudsen diffusivities is such that K is inversely proportional to $\sqrt{M}$. To examine this dependence, Knudsen diffusivities shown in Tables 2, 3, and 4 have been plotted against the recip-

Table 4. Mean Darcy Permabilities and Standard Deviations from Permeability

Particle Grade	10^7 × Mean Permeability/Std. Dev., mm²	
	Permeability Experiment	Nonisobaric Diffusion
SA203	3.23 ± 6.4%	3.13
LA617	0.076 ± 6.5%	0.083 ± 8.4%
LA622	0.523 ± 1.8%	0.481 ± 10.9%
LA623	0.928 ± 3.8%	0.958 ± 13.0%

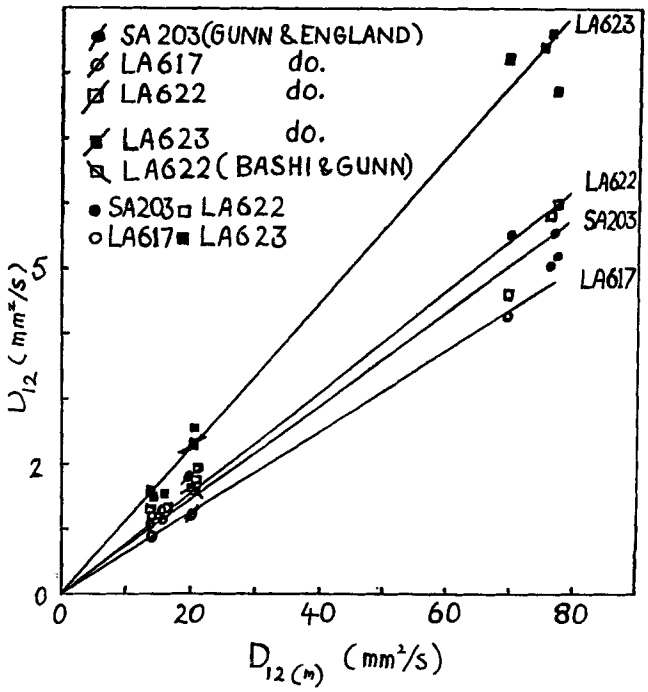

Figure 6. Dependence of effective binary diffusivity upon molecular binary diffusivity.

rocal of $\sqrt{M}$, as shown in Figure 7. A close linear dependence is shown in Figure 7, confirming the form of Eq. 3 and reinforcing estimates of the Knudsen diffusivity based upon Eq. 3 and the mean pore radii given in Table 1.

A further point of interest arises in a comparison of tortuosities calculated for the porous substrates from the effective diffusivities and porosities by Eq. 29 for bulk diffusion, and from Eq. 30 for Knudsen diffusion,

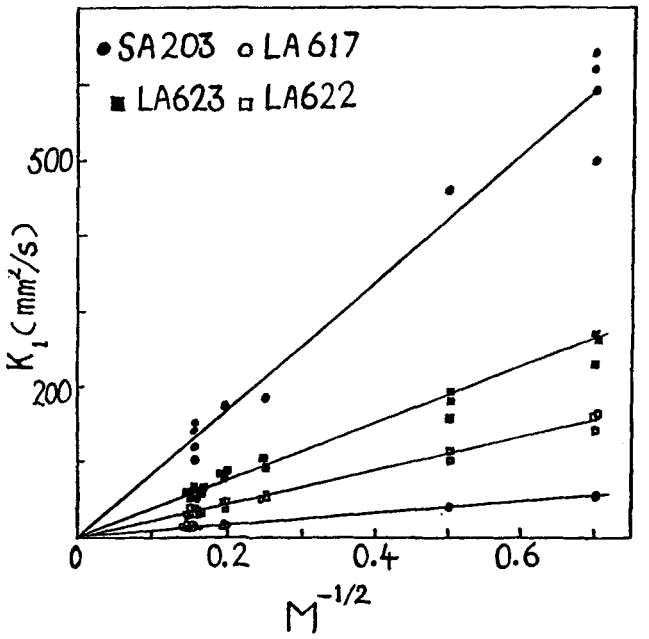

Figure 7. Dependence of effective Knudsen coefficient K_1 upon $1/\sqrt{M}$.

Table 5. Bulk Diffusion and Knudsen Tortuosities for Porous Substrates

	Gas						Mean	
Substrate	H_2	He	N_2	CH_4	Ar	CO_2	Knudsen Flow	Isobaric Diffusion
LA623	5.58	5.92	5.21	4.94	5.35	5.34	5.39	5.27
LA622	6.14	6.89	5.75	6.88	6.27	6.38	6.36	6.99
LA617	9.23	9.25	—	—	9.17	9.31	9.24	7.60
SA203	5.41	—	—	5.63	5.50	—	5.51	5.14

$$K_1 = \frac{\epsilon}{\tau}\frac{2}{3}\bar{r}\sqrt{\frac{8RT}{\pi M_1}} \tag{30}$$

where Eq. 30 without ϵ/τ gives the Knudsen diffusivity for a capillary tube of radius $\bar{r}$. Tortuosities calculated for bulk diffusion and for Knudsen diffusion are shown in Table 5. The tortuosities agree within apparent limits of experimental error for substrates LA623, LA621, and SA203. It appears, however, that the Knudsen tortuosity for LA617, the substrate with the finest pores, is significantly larger than the bulk diffusion tortuosity. This may well have some bearing upon departures from the transition relationship, Eq. 24, found particularly at low pressures, and particularly for LA617.

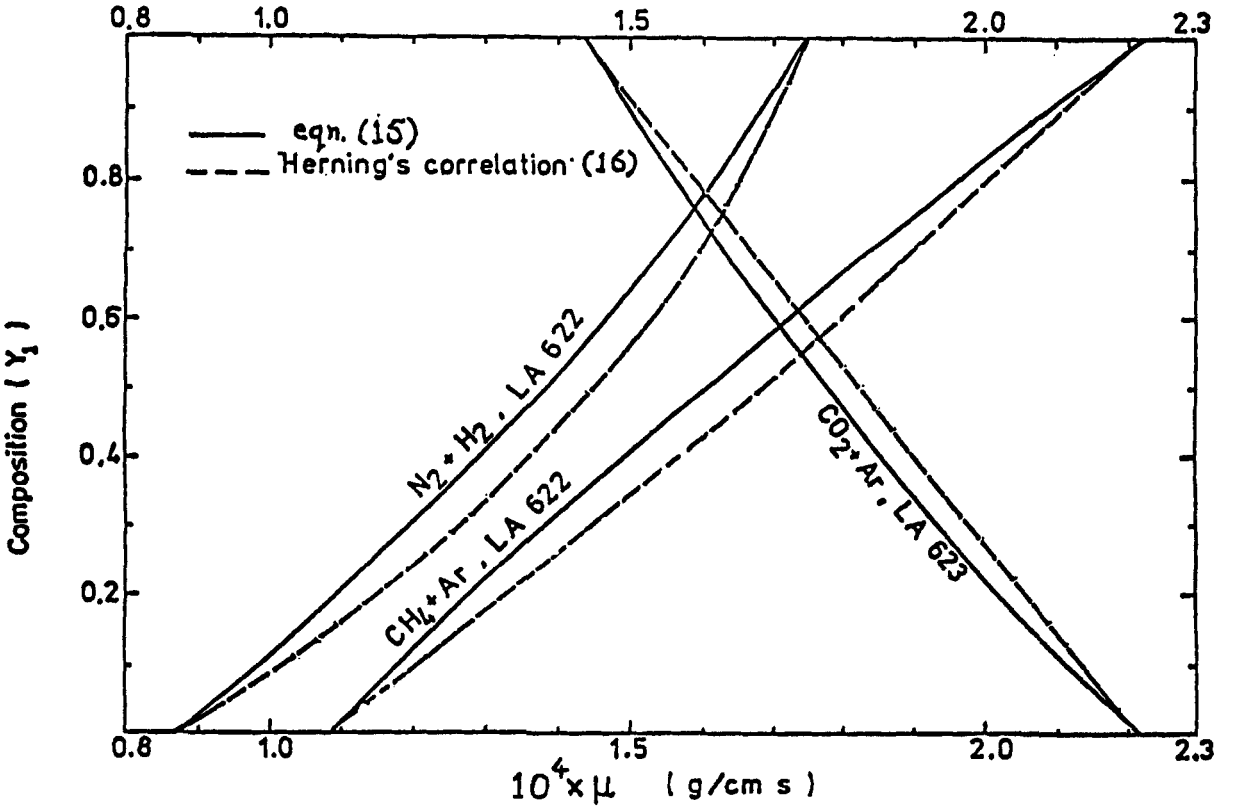

Figure 8. Comparison of Eq. 15 with Herning's Eq. 16 for viscosity of gas mixture.

There is a further comparison of interest that can be made. The differential Eqs. 11 and 12 were integrated when Eq. 16 was used to describe the concentration dependence of the viscosity for the gas mixture. Figure 8 shows the comparison between values of the gas viscosity predicted by Herning's Eq. 16 and Eq. 15 for mixtures of nitrogen and hydrogen, methane and argon, and carbon dioxide and argon. The figure shows that variations of viscosity within the pellet during forced flow and diffusion would have been highly significant, with variations of 2:1 in viscosity in some cases. It is also clear that Eq. 16 gives an estimate of the mixture viscosity that is close to Eq. 15, so providing strong support for the basis of the integration, and the subsequent interpretation of experiments on mixed diffusion and flow.

Notation

A_1, A_2, B_1, B_2, a, b = constants, Eqs. 17, 18
C = Darcy permeability
D_i = effective diffusion coefficient in transition range for component i
D_{12} = effective binary diffusivity in pellet
$D_{12(m)}$ = binary molecular diffusivity
F = sum of squares, Eq. 28
J_i = diffusive molar flux of component i
$J_{i(V)}$ = viscous molar flux of component i
$J_{i(T)}$ = total molar flux of component i
K_i = Knudsen diffusivity of component i
L = pellet thickness
M_i = relative molecular mass of component i
P = pressure
$\bar{P}$ = mean pressure
P_i = partial pressure
R = gas constant
r = pore radius
T = absolute temperature
V = pore volume
X = space coordinate
y_i = mole fraction of component i
$y_{i(j)}$ = mole fraction of component i at pellet face j
ϵ = particle porosity
μ_i = viscosity of component i
τ = tortuosity

Literature cited

Abed, R., and R. G. Rinker, "Isobaric Diffusion, Permeability and Simultaneous Flow and Diffusion in Commercial Catalysts," *J. Catal.*, **34,** 246 (1974).

Asaeda, M., J. Watanabe, Y. Matino, K. Kojima, and R. Toei, "Combined Surface and Gas Phase Diffusion through Plugs of Porous Adsorbent in Transition Region Diffusion," *J. Chem. Eng. Japan,* **14,** 13 (1981).

Barrer, R. M., "Diffusion in Porous Media," *Appl. Mater. Res.*, **2,** 129 (1963).

Bashi, H., and D. J. Gunn, "The Characterization of Fixed Beds of Porous Solids from Pulse Response," *AIChE J.*, **23,** 40 (1977).

Brownlee, K. A., *Industrial Experimentation,* Chemical Pub. Co., New York (1953).

Chen, O. T., and R. G. Rinker, "Modification of the Dusty Gas Equation to Predict Mass Transfer in Porous Media," *Chem. Eng. Sci.*, **34,** 51 (1979).

England, R., "Dispersion and Diffusion in Fixed Beds," Ph.D. Thesis, Univ. Wales (1971).

Evans, R. B., G. M. Watson, and E. A. Mason, "Gaseous Diffusion in Porous Media at Uniform Pressure," *J. Chem. Phy.*, **35,** 2076 (1961).

Gunn, D. J., and R. England, "Dispersion and Diffusion in Beds of Porous Particles," *Chem. Eng. Sci.*, **26,** 1413 (1971).

Gunn, R. D., and C. J. King, "Mass Transport in Porous Materials Under Combined Gradients of Composition and Pressure," *AIChE J.*, **15,** 507 (1969).

Mason, E. A., A. P. Malinauskas, and R. B. Evans, "Flow and Diffusion of Gases in Porous Media," *J. Chem. Phys.*, **46,** 3199 (1967).

Otani, S., N. Wakao, and J. M. Smith, "Significance of Pressure Gradients in Porous Materials. II: Diffusion and Flow in Porous Catalysts," *AIChE J.*, **11,** 439 (1965).

Pollard, W. G., and R. D. Present, "On Gaseous Self-Diffusion in Long Capillary Tubes," *Phys. Rev.*, **73,** 762 (1948).

Reid, R. C., J. M. Prausnitz, and T. K. Sherwood, *The Properties of Gases and Liquids,* McGraw-Hill, New York (1975).

Reid, R. C., and T. K. Sherwood, *The Properties of Gases and Liquids,* McGraw-Hill, New York (1958).

Satterfield, C. N., and P. J. Cadle, (1968), "Gaseous Diffusion and Flow in Commercial Catalysts at Pressure Levels Above Atmospheric," *Ind. Eng. Chem. Fundam.*, **7,** 202 (1968).

Scott, D. S., and F. A. L. Dullien, "Diffusion of Ideal Gases in Capillaries and Porous Solids," *AIChE J.*, **8,** 113 (1962).

Manuscript received Feb. 20, 1986, and revision received Oct. 27, 1986.